

Preparation of SnO₂-Sb₂O₅ films by the spray pyrolysis technique

B. CORREA-LOZANO, CH. COMNINELLIS*, A. DE BATTISTI†

Institute of Chemical Engineering, Swiss Federal Institute of Technology, CH-1015 Lausanne, Switzerland

Received 10 February 1995; revised 18 July 1995

Spray pyrolysis has been widely used for the preparation of thin ($\sim 0.1 \mu\text{m}$) and transparent SnO₂ films on glass substrates. In the present paper the parameters of the spray pyrolysis for the preparation of thick SnO₂-Sb₂O₅ conductive films on Ti substrates have been studied for electrochemical use. It has been found that the resistivity of the films exhibits a minimum for a Sb concentration of about 3 at % (precursor solution concentration) and for a preparation temperature of 550 °C. As far as the composition is concerned, it has been shown that the antimony concentration in the oxide films is about twice as large as that in the corresponding precursor solution. The dependence of the oxide loading on the substrate temperature and nature and the influence of the spray conditions have also been discussed.

1. Introduction

The literature on dimensionally stable anodes (DSA[®]) [1–3] shows that the nature of the oxide coating influences strongly their electrochemical behaviour. Although electrodes based on RuO₂ and TiO₂ are widely used in chlor-alkali cells, electrodes based on IrO₂ and Ta₂O₅ can be used for oxygen evolution in sulfuric acid media [4–6]. The case of SnO₂, in the context, is quite interesting, its role ranging between that of minor component in some DSA[®] materials, and that of main component in SnO₂-Sb₂O₅ film electrodes, of interest in electrochemical combustion of organics [7–10].

In the frame of a comprehensive research on the subject, in the present paper the spray pyrolysis technique for the preparation of SnO₂-based electrodes is studied. This technique allows a better reproducibility and better control of the preparation conditions making any attempt of correlation between final properties and preparation parameters more reliable.

SnO₂ films can be produced by means of a number of methods: for example, chemical vapour deposition (CVD), reactive sputtering and spray pyrolysis [11, 12], the last of these being the most commonly used. The effects of spraying conditions (preparation temperature, composition of the spray solution, hydrodynamics of the spray system) on the structural and electrical properties of these films have been investigated for the preparation of thin ($\sim 0.1 \mu\text{m}$) and transparent SnO₂ films on glass substrate [13].

In this work the aim was to prepare thick (2–5 μm) and conductive SnO₂-based films on titanium substrate, to be used as DSA[®]-type anodes. Some theoretical aspects of the spray pyrolysis and its application for SnO₂ films are also discussed.

2. Model treatment of the spray pyrolysis method

Figure 1 shows a simplified scheme of the spray pyrolysis technique. Although simple from an operative point of view, the spray pyrolysis method involves heat and mass transfer under unsteady conditions for the drops moving towards the substrate. These phenomena result in changes of droplet size and composition, and affect the precursor reaction.

The changes that the drops undergo after formation, can be summarized as follows: (i) changes in temperature, due to the temperature gradient between nozzle and substrate surfaces; (ii) changes in velocity, due to aerodynamic drag; and (iii) changes in size and composition caused by evaporation.

The extent to which these transformations take place depends on the geometry of the equipment, the nature and flow rate of the carrier gas and of the precursor solution and finally on the temperature profile between nozzle and substrate.

The description of the formation of thick films based on tin dioxide by the spray pyrolysis method, therefore requires appropriate modelling of the transformations that aerosol drops undergo while approaching the substrate surface. The subject can be divided as follows:

- (i) Formation of the drops at the nozzle exit, and evaluation of their mean size.
- (ii) Quantification of the evaporation during the displacement of the aerosol drops.
- (iii) Quantitative description of the drop evaporation at the substrate surface.
- (iv) Decomposition of the precursor salt(s) at the substrate surface.

A detailed study of these aspects has been carried out [14]. We will take into consideration only some aspects of the reactions of precursors at the substrate surface.

* To whom correspondence should be addressed.

† Permanent address: Department of Chemistry of the University of Ferrara, Italy.

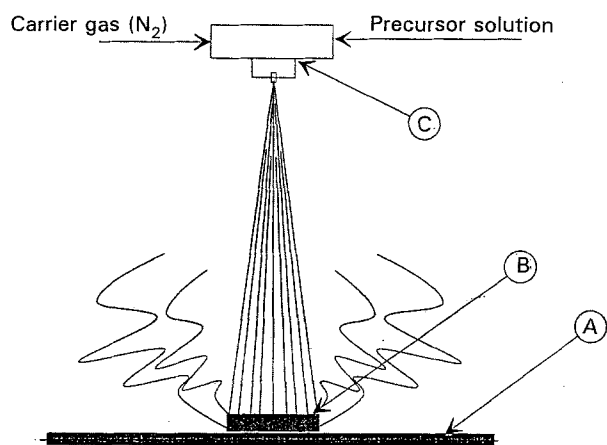
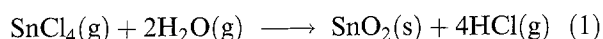


Fig. 1. Simplified scheme of the spray pyrolysis technique. (A) Heated plate; (B) substrate; (C) nozzle.

When the aerosol drops approach the heated substrate surface, under suitable experimental conditions the vapour film formed around the drop prevents direct contact between the liquid phase and the substrate surface. This occurs above a certain temperature, called the Leidenfrost temperature [15]. The evaporation of the drops in the vicinity of the support allows a continuous renewal of the vapour in the reaction layer. The decomposition reaction of SnCl_4 is a gas-phase endothermal hydrolytic reaction occurring at the substrate surface [16]:



In fact, the deposition process can be described as consisting of two stages: the reactant transport and the chemical reaction at the substrate surface.

If the whole process is controlled by reactant transport, the rate of the chemical reaction must be comparatively large, and the vapour phase concentration of SnCl_4 at the substrate surface can be taken as zero. The rate of SnO_2 formation can then be written as

$$V_f = k_g[\text{SnCl}_4]\text{B}(\text{g}) \quad (2)$$

where k_g is the mass transport coefficient and $[\text{SnCl}_4]\text{B}(\text{g})$ is the bulk concentration of tin tetrachloride in the vapour phase.

If the chemical reaction at the substrate surface is slow and in the presence of excess H_2O , the reaction should be of the first order with respect to SnCl_4 and zeroth order with respect to H_2O . The rate of deposition of the SnO_2 film becomes:

$$V_f = k_s[\text{SnCl}_4]_s(\text{g}) \quad (3)$$

where k_s is the heterogeneous reaction rate constant and $[\text{SnCl}_4]_s(\text{g})$ is the tin salt concentration in the vapour phase at the substrate surface.

Increase of the substrate temperature is expected to increase the rate of reaction. Accordingly, at sufficiently high temperatures, the whole process may become controlled by reactant transport to the substrate surface.

3. Experimental details

A simplified scheme of the spray pyrolysis equipment is given in Fig. 1. and some details are shown in Figs 2 and 3.

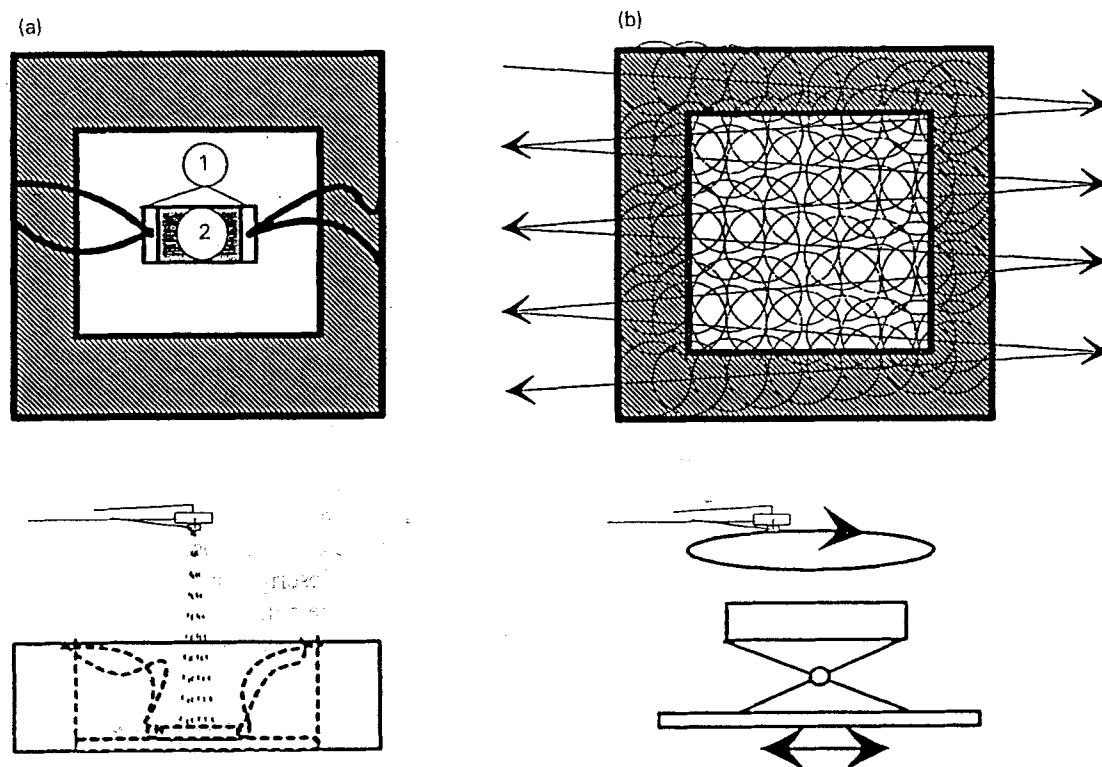


Fig. 2. Deposition of SnO_2 by spray pyrolysis. (a) Temperature measurement: (1) thermocouples; (2) substrate. (b) Spray distribution (circle represent the displacement of the spray jet).

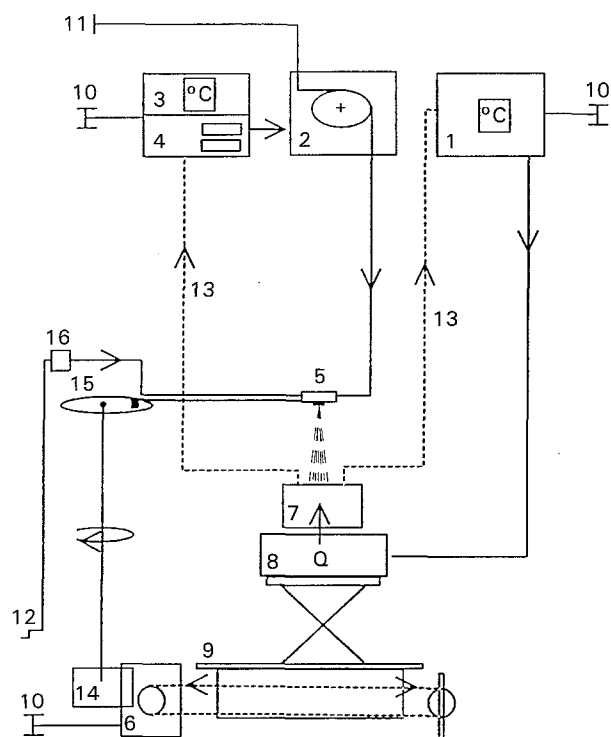


Fig. 3. Setup of the spray pyrolysis system. (1) Temperature controller; (2) peristaltic pump; (3) temperature switch; (4) chronometer (effective spraying and total time); (5) spray nozzle; (6) motor for lateral and circular displacement; (7) heating chamber; (8) heating plate; (9) lateral displacement support; (10) electrical connection; (11) spray solution; (12) carrier-gas (N_2); (13) connection to thermocouples; (14) transmission gear; (15) rotating system and nozzle support; (16) flow-meter for the carrier gas (N_2).

For a homogeneous distribution of the precursor solution aerosol all along the surface of the substrate, the spray nozzle was assigned a circular movement, whose effect combines in a synchronous way with a lateral movement of the heating plate (Fig. 2(b)).

A custom-made Ti-nozzle, replicating a SU J4B-SS model (Spraying System Co., USA) was used. This type of nozzle avoids mixing of the precursor solution and carrier-gas in its inner part.

The precursor solution was conveyed to the nozzle by a peristaltic pump (ISMATEC MV-CA-4) and N_2 (Carba gas, purity $\geq 99.5\%$) was used as carrier gas. The substrate temperature was measured by two thermocouples (Fig. 2(a)) and was maintained by means of a heating plate consisting of a heating element EGO (model 60.12160.010 1200 W 380 V) and of a digital temperature controller RCK Instruments Inc. (PID type, model RKC-REX-F7), with an average deviation of $\pm 1^\circ\text{C}$ in the temperature range 300–600 $^\circ\text{C}$. The spraying of the precursor solution on the heated substrate was regulated in such a way that the substrate temperature does not deviate from the fixed value more than 0.5%. This was achieved by a custom-built equipment (Fig. 3).

To measure the resistivity of the films (deposited on quartz), golden wires were soldered at the four corners of the sample by means of a gold paint (Demetron 8400-0040, with a gold content of 60%) [14]. During deposition, resistivity data relative to the six possible

paths between wires were collected through an Ohm-meter (Metex M-3650CR with analogic output and six-channel multiplexer) equipped with acquisition board (Analog Devices RTI-815).

The temperature profile between nozzle and substrate was determined by positioning fourteen thermocouples along the path between spray nozzle and substrate.

The reactants used for the sample preparation were: $\text{SnCl}_4 \cdot 5\text{H}_2\text{O}$ (Aldrich, 24,267-8), SbCl_3 (Fluka, 10775), HCl 32% (Fluka, 84420), Ethanol (Fluka, 02850). Both quartz and Ti plates were used as substrate.

The concentration of the tin precursor : $\text{SnCl}_4 \cdot 5\text{H}_2\text{O}$, was fixed at 10% (w/v). The solvent was an ethanol/hydrochloric acid mixture and the SbCl_3 concentration was adjusted to obtain the desired Sb atomic percentage ratio in the mixture. The determination of the deposition efficiency, η , defined as the ratio between the amount of deposited oxide and the total amount of oxide sprayed as precursor in a given time, was carried out gravimetrically by deposition on 10 cm \times 10 cm Ti plates.

4. Results and discussion

4.1. Characterization of the spray pyrolysis equipment

Figure 4 shows the shape of the temperature profiles under steady state conditions, and for three different carrier gas flows. The substrate (Ti) temperature was maintained at 550 $^\circ\text{C}$.

The temperature profile between nozzle and substrate can be represented by the dimensionless relation:

$$\frac{T}{T_{\max}} = A \left(\frac{x}{h} \right)^\alpha (Re)^\beta \quad (4)$$

where x is the distance from the substrate surface, h is the distance between substrate surface and nozzle, Re is the Reynold number for the carrier gas (N_2) at the nozzle exit. A , α , β are phenomenological constants

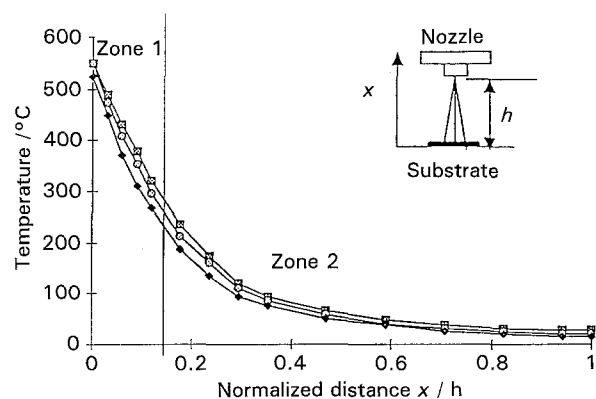


Fig. 4. Temperature profiles between substrate and nozzle, at different carrier gas (N_2) flows. $h = 170$ mm. Key: (— \square —) 16.6, (— \circ —) 50 and (— \blacklozenge —) 66.6 cm^3s^{-1} .

and T_{\max} is the temperature at the substrate surface. Under constant flow conditions ($Re = \text{const}$):

$$\frac{T}{T_{\max}} = A\alpha\left(\frac{x}{h}\right)^{\alpha} \quad (5)$$

or

$$\ln\left(\frac{T}{T_{\max}}\right) = \ln A' + \alpha \ln\left(\frac{x}{h}\right) \quad (6)$$

The values of the constant A' and α can be determined experimentally. (Fig. 5) For low distances from the substrate (zone 1, in Fig. 5), values of 0.303 and -0.311 were found for A' and α , respectively, for larger distances (zone 2, in Fig. 5) $A' = 0.042$ and $\alpha = -1.268$.

4.2. Preparation of the $\text{SnO}_2\text{-Sb}_2\text{O}_5$ films

4.2.1. Influence of antimony concentration on the film resistivity. $\text{SnO}_2\text{-Sb}_2\text{O}_5$ mixed oxide films were prepared on quartz substrates, from precursor solutions with different Sn/Sb ratios. The resistivity of the films at 25°C was measured by the method described in the experimental part. The results as a function of the Sb concentration in the precursor solution, are shown in Fig. 6. It can be observed that the film resistivity rapidly decreases for small Sb additions, reaching a shallow minimum around 3 at% of Sb (precursor solution composition corresponding to about 6 at% in the oxide film). This result is in good agreement with the literature [8, 17–19]. In order to verify the film composition and attempt direct correlations with the antimony content in the films, XPS and EDS characterization of the samples was carried out. The results indicate the antimony/tin atom ratio in the films is larger than in the respective precursor solution of at least a factor of two [14].

4.2.2. Influence of the substrate temperature on the film resistivity. Figure 7 shows the effect of the preparation temperature on the resistivity of $\text{SnO}_2\text{-Sb}_2\text{O}_5$ films (3 at% Sb in the precursor solution), measured at

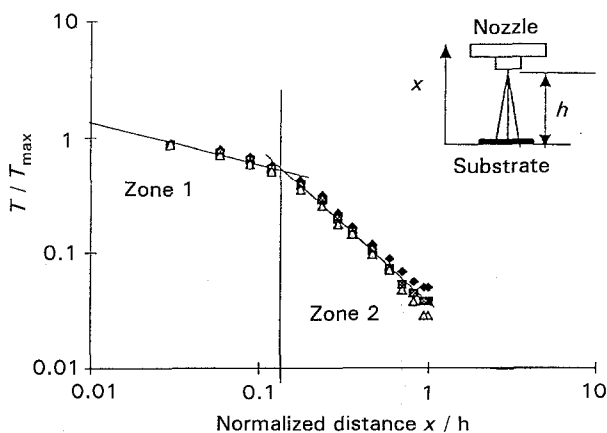


Fig. 5. Temperature profile between substrate and nozzle. Graphical representation of Equation 6, conditions. Key as for Fig. 4.

25°C . A flat minimum is observed at 550°C . The decrease between 400 and 550°C can be related to a better Sb(V) insertion in the SnO_2 crystallites. XPS results indicate that, when the preparation temperature is kept below 500°C , no Sb species can be detected in films prepared from precursor solutions containing 3 at% Sb [14]. Another possible factor which may contribute to the initial decrease of resistivity, is the increase of the number of defects (oxygen deficiency) which accompanies the increase in the preparation temperature [14]. Most probably both factors contribute to the observed trend.

4.2.3. Dependence of the oxide loading rate on the deposition temperature and substrate nature. Spray pyrolysis preparations on quartz and titanium substrates were carried out at nine different temperatures, between 350 and 750°C . The amount of oxide loading has been followed gravimetrically. Below 350°C no oxide deposition was observed. On the other hand, for deposition temperatures higher than 570°C , on titanium substrates the rate of formation of TiO_2 became large [20], causing poor adhesion of the SnO_2 film. Accordingly, as far as the preparation of SnO_2 -based electrodes is concerned, the temperature region above 570°C is of limited interest. As shown in Fig. 8, for the case of quartz supports, allowing a more reliable investigation in

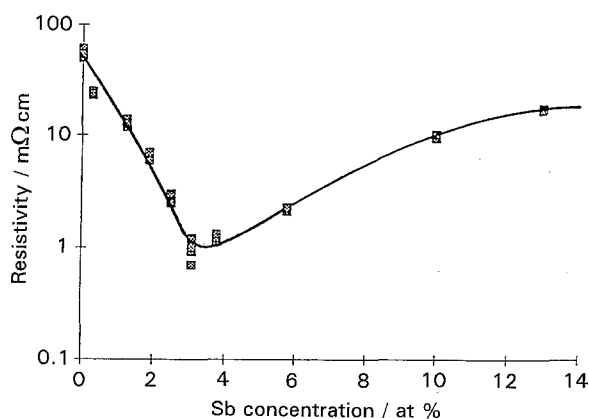


Fig. 6. Dependence of the resistivity of $\text{SnO}_2\text{-Sb}_2\text{O}_5$ films measured at 25°C on Sb concentration in the precursor solution. Deposition temperature: 550°C ; substrate: quartz.

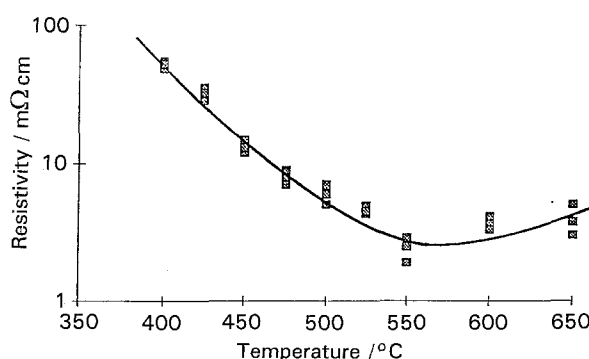


Fig. 7. Dependence of resistivity of a $\text{SnO}_2\text{-Sb}_2\text{O}_5$ film (3 at% Sb in the precursor solution) measured at 25°C on the deposition temperature, substrate: quartz.

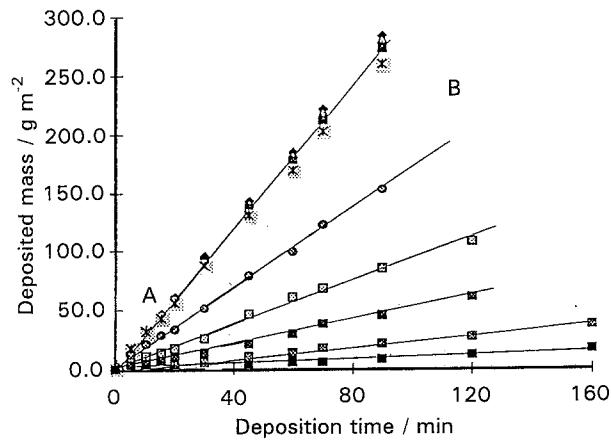


Fig. 8. Mass of deposited SnO₂-Sb₂O₅ (3 at % Sb in the precursor solution) as a function of spray time, at different deposition temperatures. The substrate was quartz. The precursor solution flow was 1.86 cm³ min⁻¹. Key: (◇, △, □, ⊠) 750 °C, 700 °C, 650 °C, 600 °C (top curve); (○) 550 °C; (□, ⊠, ⊞, ■) 500 °C, 450 °C, 400 °C, 350 °C (lower four curves).

wider temperature ranges, at constant deposition time the oxide loading increases with the deposition temperature. On the other hand, when a given temperature is reached, the deposition rate becomes constant, after an initial decrease (Fig. 9).

The result in Fig. 9 can then be explained by the assumption that initially, when the quartz surface is only partially covered, the deposition rate is affected by the nature of the substrate surface. After a certain critical loading level is reached, further deposition takes place on a more or less homogeneous SnO₂ substrate. In Fig. 10 the logarithm of deposition rate, V_r , has been plotted against the reciprocal of the substrate temperature. Two regions can be identified in the plot. In region A, V_r is linear in T^{-1} , while substantial independence between the two variables is observed above a given temperature (region B). From the slope of the first part of the plot an activation energy of 2.68 kJ mol⁻¹ was evaluated, in very good agreement with the literature, indicating a value of 2.75 kJ mol⁻¹ [21]. The evidence obtained in Fig. 10, confirms kinetic control by the chemical step in the deposition process at low temperatures (< 600 °C) and reactant transport at high temperatures (> 600 °C).

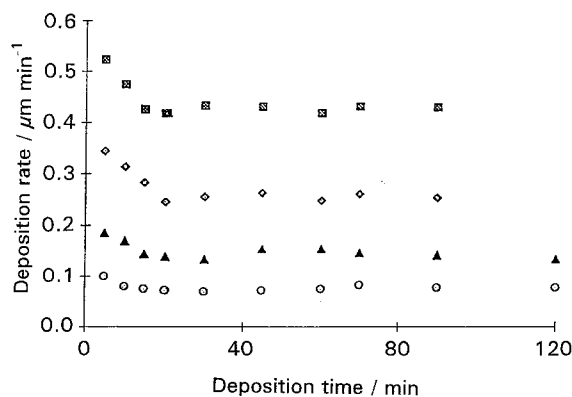


Fig. 9. Dependence of the SnO₂-Sb₂O₅ deposition rate on the deposition time, at constant deposition temperature. conditions as in Fig. 8. Key: (⊠) 600 °C, (◇) 550 °C, (▲) 500 °C and (⊙) 450 °C.

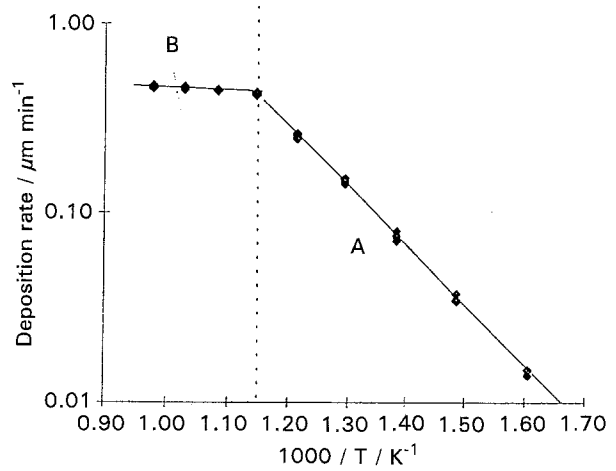


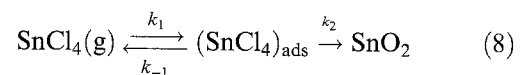
Fig. 10. Dependence of the logarithm of the deposition rate ($\mu\text{m min}^{-1}$) of SnO₂-Sb₂O₅ film (3 at % Sb in the precursor solution) on the reciprocal of the deposition temperature.

4.2.4. Dependence of the oxide loading on the precursor solution flow rate. As already discussed in the introduction, thick SnO₂-based films deserve particular attention for their potential use as DSA[®]-type electrodes. A specific problem to be taken into account in the preparation of this type of device is that, when trying to reach larger thicknesses, detachment of the deposit from the substrate may take place during the cooling stage. In the case of Ti, substrate usually used for electrodic devices, the loss of adhesion depends not only on the film thickness, but also on the flow of the precursor solution. Typically, at a preparation temperature of 550 °C, the oxide loading cannot exceed 40 g m⁻², at a precursor solution flow of 0.7 ml min⁻¹, while at a solution feed of 1.86 ml min⁻¹, the limiting loading allowed, before detachment phenomena appear, is 100 g m⁻². This can be explained assuming that under prolonged heating at the given temperature, extensive oxidation of the titanium support becomes important. This would certainly favour the detaching action of the mechanical stresses active at the oxide/substrate interface.

Optimization of the preparation of Ti-supported tin dioxide films therefore requires an investigation of the optimal precursor solution flows, and oxide loading. Figure 11 shows the dependence of the loading rate V_r on the precursor solution flow, q , at a substrate temperature of 550 °C. The relation between the two variables can be satisfactorily expressed as

$$V_r = \frac{V_m q}{K_s + q} \quad (7)$$

where V_m represents the maximum deposition rate. This equation is in agreement with the mechanism:



with $K_s = (k_{-1} + k_2)/k_1$.

According to this mechanism SnCl₄ is absorbed from

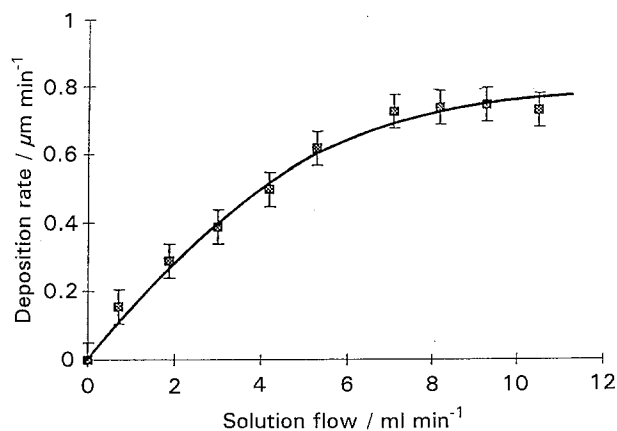


Fig. 11. Deposition rate of $\text{SnO}_2\text{-Sb}_2\text{O}_5$ film (3 at% Sb in the precursor solution) as a function of the solution flow. Carrier gas(N_2) flow: $3 \text{ cm}^3 \text{ min}^{-1}$. Deposition temperature: 550°C ; substrate: Ti.

the gas phase to the substrate surface where it is hydrolysed to SnO_2 .

An important parameter, that allows the evaluation of the efficiency of the spray pyrolysis equipment is the deposition yield (η) (see Experimental details). The dependence of η on the solution flow for a $10 \text{ cm} \times 10 \text{ cm}$ Ti plates is shown in Fig. 12. It can be observed that η decreases with increasing solution flow, in agreement with the deposition mechanism proposed.

4.2.5. Changes of the film resistivity during the deposition process. Results on the influence of the oxide loading on the resistivity of $\text{SnO}_2\text{-Sb}_2\text{O}_5$ films (3 at% Sb in the precursor solution; preparation temperature 550°C) deposited on quartz are shown in Fig. 13. A first fast decrease with increasing the oxide loading is observed. A minimum value is reached around a thickness of $8 \mu\text{m}$ (tin oxide loading: 48 g m^{-2}). This trend may be due to the reaction of the oxide film with ethanol (component of the solvent mixture) which acts as reducing agent, changing the oxide stoichiometry and resulting in

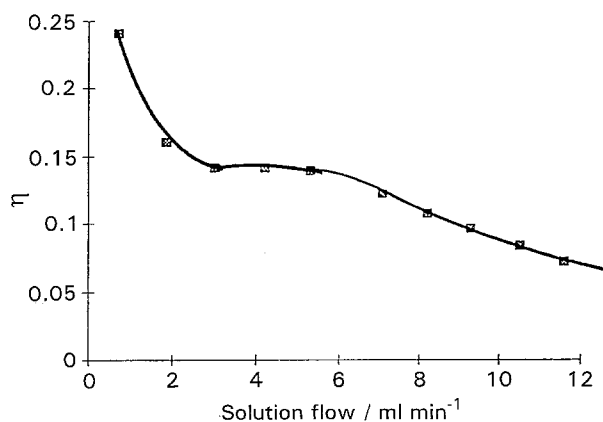


Fig. 12. Deposition yield (η) of $\text{SnO}_2\text{-Sb}_2\text{O}_5$ film (3 at% Sb in the precursor solution) as a function of solution flow. Deposition temperature: 555°C ; substrate: Ti.

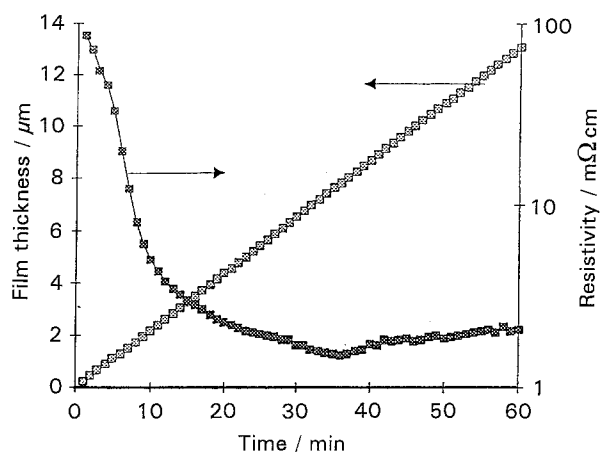


Fig. 13. Influence of oxide loading on coating resistivity.

oxygen deficiency in the films. Doping with chloride ions can also explain the observed behaviour.

An important factor which negatively influences the electrical transport in thicker films is the formation of cracks during the cooling stage subsequent to the preparation (Fig. 14). The phenomenon is observed only for loadings larger than 6 g m^{-2} (a thickness of about $1.0 \mu\text{m}$). The crack formation does not seem to be affected by the substrate nature.

5. Conclusion

Preparation of $\text{SnO}_2\text{-Sb}_2\text{O}_5$ films by spray pyrolysis has shown that:

- (i) The spray pyrolysis technique, compared with the sol-gel, more traditional for oxide electrode preparation, has the considerable advantage of a much more clearcut definition of the preparation parameter, and of more quantitative control.
- (ii) The Sb concentration in the oxide film is larger than in the precursor solution, by a factor of about 2, probably due to a larger deposition rate of antimony oxide.
- (iii) The resistivity of $\text{SnO}_2\text{-Sb}_2\text{O}_5$ films exhibits a minimum for a deposition temperature around 550°C .

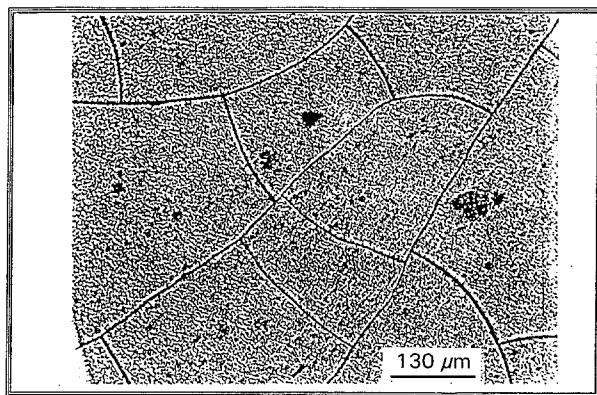


Fig. 14. SEM micrograph showing cracks at the surface of a $\text{SnO}_2\text{-Sb}_2\text{O}_5$ film (3 at% Sb in the precursor solution), substrate: quartz, deposition temperature: 550°C ; thickness: $5.3 \mu\text{m}$.

(iv) In the case of titanium-supported films, interesting for the electrochemical applications, the duration of the deposition has to be kept at a minimum, by increasing the precursor solution flow.

(v) The spray pyrolysis method, allows deposition rates as high as 0.8 μm min⁻¹.

References

- [1] S. Trasatti and G. Lodi, in 'Electrodes of conductive metal oxides', (edited by S. Trasatti), Elsevier, Amsterdam (1980) Part A, p. 301.
- [2] *Idem*, in *ibid.* (1981) Part B, p. 521.
- [3] S. Trasatti and W. E. O'Gready, in 'Advances in electrochemistry and electrochemical engineering', Vol. 12, (Edited by H. Gerischer and C. W. Tobias), Wiley, New York (1981) p. 177.
- [4] J. Rolewicz, Ch. Comninellis, E. Plattner and J. Hinden, *Chimia* **42** (1988) 75.
- [5] J. Rolewicz, Ch. Comninellis, E. Plattner and J. Hinden, *Electrochim. Acta* **33** (1988) 573.
- [6] G. P. Vercesi, J.-Y. Salamin and Ch. Comninellis, *ibid.* **36** (1991) 991.
- [7] R. Kötzt, S. Stücker and B. Carcer, *J. Appl. Electrochem.* **21** (1991) 14.
- [8] S. Stücker, R. Kötzt, B. Carcer and W. Suter, *J. Appl. Electrochem.* **21** (1991) 99.
- [9] Ch. Comninellis and C. Pulgarin, *ibid.* **23** (1993) 108.
- [10] Ch. Comninellis, *Electrochim. Acta* **39** (1994) 1857.
- [11] H. C. MacMaster, *British Patent* 632 (1942).
- [12] J. C. Manificier, M. de Murcia and J. P. Fillard, *Mat. Res. Bull.* **10** (1975) 1215.
- [13] W. E. Ranz and W. R. Marshal, *Chem. Eng. Progr.* **48** (1952) 141.
- [14] B. Correa-Lozano, EPFL, Thèse 1297 (1994), Lausanne, Switzerland.
- [15] B. S. Gotteried, C. J. Lee and K. L. Bell, *J. Heat, Mass Transf.* **9** (1968) 1167.
- [16] W. M. Sears and M. A. Gee, *Thin Solid Films* **165** (1988) 265.
- [17] E. Shantthi, A. Banerjee and K. L. Chopra, *ibid.* **88** (1982) 93.
- [18] S. K. Sing and S. Basu, *Mater. Chem. Phys.* **20** (1988) 381.
- [19] F. C. Stedile, C. V. Barros Leite, W. H. Schreiner and J. R. Baumvol, *Thin Solid Films* **190** (1990) 139.
- [20] G. P. Vercesi, J. Rolewicz, Ch. Comninellis and J. Hinden, *Thermochim. Acta* **176** (1991) 31.
- [21] J. Sanz Maudes and T. Rodriguez, *Thin Solid Films* **69** (1980) 183.